Regional heterogeneity of D2-receptor signaling in the dorsal striatum and nucleus accumbens

Pamela F Marcott[1,2], **Sheng Gong**[1,2], **Prashant Donthamsetti**[3,4], **Steven G. Grinnell**[8,9], **Melissa N. Nelson**[8,9], **Amy H Newman**[5], **Lutz Birnbaumer**[6], **Kirill A Martemyanov**[7], **Jonathan A Javitch**[3,8,9], and **Christopher P Ford**[1,2,*]

[1]Department of Pharmacology, University of Colorado School of Medicine, Anschutz Medical Campus, Aurora, CO 80045, USA

[2]Department of Physiology and Biophysics, Case Western Reserve University School of Medicine, Cleveland, OH 44106, USA

[3]Department of Pharmacology, Columbia University, New York, NY 10032, USA

[5]National Institute of Drug Abuse -Intramural Research Program, NIH, Baltimore MD,21224, USA

[6]Neurobiology Laboratory, National Institute of Environmental Health Sciences, North Carolina 27709, and Institute of Biomedical Research (BIOMED), Catholic University of Argentina, Buenos Aires C1107AAZ, Argentina

[7]Department of Neuroscience, The Scripps Research Institute, Jupiter, FL 33458, USA

[8]Department of Psychiatry, Columbia University, New York, NY 10032, USA

[9]Division of Molecular Therapeutics, New York State Psychiatric Institute, New York, NY 10032, USA

Abstract

Dopamine input to the dorsal and ventral striatum originates from separate populations of midbrain neurons. Despite differences in afferent inputs and behavioral output, little is known about how dopamine release is encoded by dopamine receptors on medium spiny neurons (MSNs) across striatal subregions. Here we examined the activation of D2-receptors following the synaptic release of dopamine in the dorsal striatum (DStr) and nucleus accumbens shell (NAc). We found that D2-receptor mediated synaptic currents were slower in the NAc and this difference occurred

Address for Correspondence: Department of Pharmacology, University of Colorado School of Medicine, 12800 E 19th Ave, Aurora, CO, 80045.
[4]Current address: Department of Molecular and Cell Biology, University of California, Berkeley, California 94720, USA
*Lead Contact/Corresponding author: Christopher Ford, (christopher.ford@ucdenver.edu)

at the level of D2-receptor signaling. As a result of preferential coupling to Gαo, we also found that D2-receptors in MSNs demonstrated higher sensitivity for dopamine in the NAc. The higher sensitivity in the NAc was eliminated following cocaine exposure. These results identify differences in the sensitivity and timing of D2-receptor signaling across the striatum, which influence how nigrostriatal and mesolimbic signals are encoded across these circuits.

eTOC blurb

Marcott et al identify that D2-receptors on MSNs differ in their sensitivity and rate of activation between the dorsal striatum and nucleus accumbens. These regional differences in signaling shape how D2-receptors encode dopamine release events in nigrostriatal and mesolimbic circuits.

Introduction

The striatum is the input nucleus of the basal ganglia and is involved in goal-directed behaviors, motivation, and reward processing. Subdivided into dorsal (DStr) and ventral striatum, or nucleus accumbens (NAc), these striatal subregions have different afferent and efferent connections and are involved in unique behavioral functions. The DStr receives dopamine inputs from the substantia nigra pars compacta and is primarily associated with sensorimotor functions, while the NAc receives dopamine projections from the ventral tegmental area and is more commonly associated with limbic related functions.

Dopamine transmission in the striatum has been classically studied using fast scan cyclic voltammetry (FSCV) to measure dopamine release in the extracellular space (Ewing et al., 1983). Both *in vitro* and *in vivo* studies have shown that there is a dorsal-to-ventral gradient in the magnitude of stimulated dopamine release and the kinetics of reuptake, with the highest levels of both in the DStr as compared to the NAc (Cragg et al., 2002; Jones et al., 1995). The regional heterogeneity of FSCV dopamine transients is thought to be due to differences in the density of dopamine innervation (Pacelli et al., 2015; Parent and Parent, 2006), expression of dopamine transporters (Marshall et al., 1990), and frequency dependent regulation by presynaptic nicotinic acetylcholine receptors (Rice et al., 2011; Zhang et al., 2009). In addition, drugs of abuse differentially regulate dopamine transmission across striatal subregions. Cocaine preferentially increases dopamine levels in the NAc (Di Chiara and Imperato, 1988), and self-administration studies have demonstrated that the initial rewarding effects of cocaine are predominantly due to its actions in this region (Ikemoto and Bonci, 2014). However, during the transition from voluntary to compulsive drug use, the region controlling cocaine seeking behaviors shifts to the DStr (Everitt and Robbins, 2013; Self, 2010).

Dopamine has opposing actions on medium spiny neurons (MSNs) of the direct and indirect pathways via activation of D1 and D2 receptors, respectively (Gerfen and Surmeier, 2011). Despite the regional heterogeneity of dopamine release and its involvement in unique behavioral functions in the DStr and NAc, little is known about how synaptic dopamine receptors are differentially activated throughout the striatum. In order to study regional differences in D2-receptor transmission, we utilized viral overexpression of a G-protein coupled inward rectifying potassium (GIRK) channel (Marcott et al., 2014) to directly

measure striatal D2-receptor activation in the DStr and NAc. Despite regional differences in the amount of dopamine released, we found that D2-receptors were maximally activated by the synaptic release of dopamine in both the DStr and NAc. D2-receptors of the NAc were slower to activate than those of the DStr and this difference was not due to regional differences in release or reuptake. D2-receptors of the NAc medial shell had a higher sensitivity for dopamine, which decreased in response to chronic cocaine administration. In addition, we found that this regional difference in sensitivity was seen not only for dendritic D2-receptors coupled to GIRK channels, but also at axonal D2-receptors coupled to endogenous signaling pathways regulating local GABAergic collateral transmission. We found this difference in sensitivity could be accounted for by region-specific differences in coupling to G-proteins. Together, these results demonstrate that the timing and sensitivity of D2-receptor actions are differentially subjected to fine-tuning by postsynaptic signaling molecules that differ across striatal regions.

Results

Dopamine D2-receptors encode the synaptic release of dopamine differently between striatal subregions

We first sought to verify regional differences in evoked dopamine release using fast scan cyclic voltammetry (FSCV). An AAV encoding double-floxed channelrhodopsin-2 (ChR2) was injected into the midbrain of dopamine transporter (DAT) IRES Cre mice (Figure 1A). Three weeks following stereotaxic injection, coronal brain slices were cut containing the dorsal striatum (DStr) and nucleus accumbens (NAc) (Figure 1A). Since the medial shell of the NAc is most strongly associated with psychostimulant abuse and reward processing (Ikemoto and Bonci, 2014), we focused on this subdivision of the NAc. A carbon fiber electrode was inserted into the DStr or NAc medial shell and was cycled (10 Hz) from −0.4 V to 1.3 V using a triangular waveform (400 V/s) (Figure 1B, inset). DHβE (1 μM) was included in the recording solution to block effects of presynaptic nicotinic receptors on dopamine terminals. A single pulse of wide-field blue light was used to optogenetically evoke dopamine release. When compared across regions, the peak extracellular concentration of dopamine ($[DA]_o$) was greater in the DStr than in the NAc ($p < 0.01$, Mann-Whitney test) (Figures 1B and 1C). In addition to displaying regional differences in peak $[DA]_o$, FSCV transients in the DStr and NAc also appeared to have different kinetics. In order to more carefully measure differences in the kinetics of dopamine release and clearance across striatal subregions, the FSCV waveform was altered to allow for more rapid sampling and thus greater kinetic resolution (100 Hz) (Figure 1D, inset). Using this protocol, dopamine transients displayed a similar lag to onset and rate of rise in the DStr and NAc (Figures 1D and 1E), indicating that the rate of release is similar across striatal subregions. However, dopamine transients were slower to decay in the NAc (Figure 1E). This is consistent with past electrochemical results showing a regional heterogeneity in the amount of dopamine released and rate of clearance across regions (Cragg et al., 2002; Jones et al., 1995).

We next examined how these regional differences in extracellular dopamine transients were encoded by synaptic dopamine D2-receptors on indirect pathway MSNs (D2-MSNs). To

measure the activation of striatal D2-receptors, we virally overexpressed a G-protein coupled inward rectifying potassium (GIRK2) channel in MSNs. Endogenous D2-receptors on D2-MSNs can couple to overexpressed GIRK2 channels, providing a rapid, direct readout of synaptic D2-receptor activation (Marcott et al., 2014). Since D1-receptors are G_s-coupled and do not readily couple to GIRK channels, only dopamine D2-receptors were examined. An AAV encoding GIRK2 and a soluble tdTomato fluorophore was injected into both the DStr and NAc (Figure 1A). Three weeks following viral injections, coronal brain slices were cut for electrophysiological recordings. Whole-cell voltage clamp recordings ($V_h = -60$ mV) were made from GIRK2-expressing neurons, identified by tdTomato fluorescence (Marcott et al., 2014). Neurons were classified as MSNs based on their morphological and electrophysiological properties, including a hyperpolarized resting membrane potential and low input resistance (Kreitzer, 2009). The expression of GIRK2 does not affect MSN excitability or membrane resistance (Marcott et al., 2014). Recordings were made in the presence of NMDA, $GABA_A$, $GABA_B$, muscarinic, and D1-receptor antagonists to pharmacologically isolate D2-receptor mediated GIRK currents. A single flash of blue light evoked a D2-receptor mediated inhibitory postsynaptic current (D2-IPSC) in about half of MSNs of the DStr and NAc (Figure 1F). To confirm that D2-IPSCs could only be recorded in D2-MSNs, an AAV expressing double-floxed GIRK2 and tdTomato was injected into the DStr and NAc of Adora2a-Cre (A2A-Cre) mice to target D2-receptor expressing MSNs (Supplemental Figure 1A). In both the DStr and NAc, electrical stimulation evoked D2-IPSCs in all tdTomato[+] MSNs (Supplemental Figures 1B and 1C). As there are reports of MSNs co-expressing D1- and D2-receptors, particularly in the NAc, we also drove expression of GIRK and tdTomato in D1-receptor expressing MSNs of the direct pathway (D1-MSNs) using a D1-Cre transgenic mouse (Supplemental Figure 1D). Electrical stimulation did not evoke D2-IPSCs in GIRK-expressing D1-MSNs in either the DStr or NAc (Supplemental Figure 1E), confirming that D2-IPSCs were only observed in D2-MSNs.

Since the magnitude of evoked dopamine was significantly less in NAc (Figures 1B and 1C), we sought to examine whether there was a difference in the extent of D2-receptor activation between regions. D2-IPSCs recorded in the DStr and NAc medial shell showed the same average amplitude (p = 0.99, Mann-Whitney test) (Figure 1G). The ratio of D2-IPSC amplitude to maximum outward D2-receptor mediated current (measured in response to 100 μM exogenous dopamine) was also the same in the DStr and NAc (p = 0.5, Mann-Whitney test) (Figure 1H). This suggests that, despite significantly less dopamine released into the bulk extracellular space in the NAc, the maximum level of D2-receptor activation is similar in both regions. In addition, the kinetics of D2-IPSCs of the DStr were faster than those of the NAc (Figures 1F and 1I – 1K). D2-IPSCs in the NAc medial shell were slower to activate and decay than in the DStr (p < 0.001, Mann-Whitney tests) (Figures 1I – 1K). This difference in kinetics was not due to the overall amount of dopamine released, as reducing the intensity of optical stimulation in the DStr did not slow the kinetics of D2-IPSCs in the DStr despite reducing the amplitude of IPSCs by ~60% (Supplemental Figure 1F). Thus, even with reduced release, the kinetics of D2-IPSCs in the DStr were still faster than those in the NAc evoked with maximal intensity stimulation.

Region-specific contribution of reuptake, spillover and terminal density in regulating synaptic activation of D2-receptors

The dopamine transporter (DAT) regulates the extracellular level of dopamine and DAT expression differs along the dorsal-to-ventral axis in the striatum (Rice et al., 2011). In order to eliminate the contribution of reuptake, D2-IPSCs were recorded in the presence of a near saturating concentration of the monoamine transport blocker nomifensine (10 μM) (Figure 2A). In both the DStr and NAc, nomifensine slowed the decay time of D2-IPSCs but had no effect on onset kinetics ($p = 0.5$, two-way ANOVA) (Figures 2B – 2C), suggesting that DATs do not regulate activation kinetics of IPSCs. Blocking reuptake also did not have any effect on the rate of dopamine release as measured by FSCV (Supplemental Figures 2A – 2B). The regional difference in decay kinetics was eliminated by blocking DATs with nomifensine (Supplemental Figures 2C – 2E), confirming that differences in uptake regionally regulate the duration of dopamine in the extracellular space following release (Rice et al., 2011). However, D2-IPSCs in the DStr were still faster to activate than in the NAc in the presence of nomifensine ($p < 0.01$, Mann-Whitney test) (Figures 2A – 2C). Similar results were found in the presence of cocaine (10 μM) and in DAT-knockout mice (Figure 2C, Supplemental Figures 2C – 2E). As the rate of dopamine release was similar in the DStr and NAc, these results suggest that a DAT-independent mechanism is likely responsible for the regional difference in kinetics of activation of D2-receptors across the striatum.

We next examined if differences in the extent of diffusion of dopamine could account for the regional differences in kinetics. Slowing diffusion with dextran (5% w/v) (Courtney and Ford, 2014) had a similar effect on the lag to onset and amplitude of D2-IPSCs of the DStr and NAc (Figures 2D – 2E). This suggests that dopamine diffuses a similar distance from release sites to postsynaptic D2-receptors in both striatal subregions. Likewise, activating as few release sites as possible by using minimal stimulation with a local stimulating electrode did not eliminate the regional difference in activation kinetics (Figures 2F – 2I). Lastly, to control for potential regional differences in GIRK expression, we measured D2-IPSCs in the DStr and NAc only five days following AAV.GIRK2 injection. At this early time point, GIRK expression is low and the amplitude of D2-IPSCs are small (Marcott et al., 2014) (Supplemental Figure 2F). There was no regional difference in the amplitude of D2-IPSCs and the regional difference in kinetics was already observed (Supplemental Figure 2F). While these results confirm that reuptake, spillover, and diffusion play critical roles in regulating extracellular dopamine and the resulting activation of D2-receptors, they identify that additional mechanism(s) regulate the kinetics by which D2-receptors differentially encode nigrostriatal and mesolimbic dopamine signals.

Regional differences in the kinetics of postsynaptic D2-receptor signaling

We next asked whether the regional differences in the kinetics could be attributed to differences at the level of postsynaptic D2-receptor activation. MSNs in the DStr or NAc medial shell were patch-clamped and the dendrites were imaged by 2-photon microscopy (Figure 3A). An iontophoretic pipette filled with dopamine (1 M) was placed as close as possible to a postsynaptic dendrite (within 1–2 μm) (Figure 3A). A short pulse of dopamine (2 – 5 ms) was applied to produce a minimal D2-receptor mediated GIRK current on the postsynaptic cell being recorded (Figure 3B). Minimal postsynaptic GIRK currents produced

by focal iontophoresis of dopamine were slower to rise than IPSCs evoked with minimal stimulation of dopamine terminals (Figure 3E), indicating that the concentration of dopamine at D2-receptors following iontophoresis is lower than the synaptic concentration of dopamine mediating the IPSC (Marcott et al., 2014).

Minimal postsynaptic D2-receptor mediated currents had the same amplitude between regions ($p = 0.2$, two-way ANOVA) (Figure 3C), but were always faster to rise in the DStr than in the NAc ($p < 0.05$, two-way ANOVA with Tukey's post-test) (Figures 3B and 3D). This is consistent with the findings from above using low intensity stimulation in the DStr (Supplemental Figure 1F), demonstrating that the faster rate of D2-receptor activation in the DStr likely does not result from greater release of dopamine in that region. Minimal postsynaptic GIRK currents in the DStr evoked in the presence of a low dose of cocaine (300 nM), to block about half of transporters (Jones et al., 1995), were still faster than in the NAc under control conditions ($p < 0.05$, two-way ANOVA with Tukey's post-test) (Figure 3B – 3D). This result suggests that D2-receptors of the NAc have intrinsically slower activation kinetics than those of the DStr and again confirms that this difference is not due to regional differences in the rate of dopamine release or the extent of reuptake.

Higher concentrations of dopamine are required to activate D2-receptors of the DStr than the NAc medial shell

Since regional differences were seen in the activation of D2-receptors, we next examined if D2-receptors in the DStr and NAc medial shell also had differences in their sensitivity to dopamine. The concentration-response relationship for dopamine was determined by bath applying different concentrations of dopamine and measuring the resulting outward GIRK current (Figures 4A and 4B). Recordings were performed in the presence of cocaine (10 μM) to block reuptake and DHβE (1 μM) to block nicotinic receptors. The EC_{50} of D2-receptor activation by dopamine in the DStr was 5.9 μM (Figure 4F and Supplemental Table 1). The concentration-response curve for D2-receptors in the NAc medial shell was shifted to the left, with an EC_{50} of 1.3 μM ($p < 0.001$, two-way ANOVA) (Figure 4F and Supplemental Table 1). There was no difference in maximum outward current (produced by 300 μM DA) between the DStr and NAc. This suggests that, despite demonstrating the same maximal level of activation, D2-receptors in the NAc have a higher sensitivity for dopamine than those of the DStr.

Dopamine neurons have pacemaker firing activity that switches to a phasic or burst firing mode in response to reward-related cues. D2-receptors are not fully saturated by low micromolar concentrations of dopamine, but rather are capable of encoding phasic signals superimposed on background tonic levels (Marcott et al., 2014). In order to examine the relationship between tonic and phasic dopamine signals in the DStr and NAc, D2-IPSCs evoked at the peak of the dopamine mediated outward current were compared to the total outward current generated (standing outward current in 3 μM dopamine + peak IPSC). Dopamine (3 μM) produced larger outward currents in the NAc and the amount of phasic D2-IPSC remaining at the peak of the standing outward current was smaller than in the DStr ($p < 0.001$, two-way ANOVA with Tukey's post-test) (Figures 4A, 4B and 4G). The results

suggest that D2-receptors of the DStr can signal with larger phasic increases superimposed on tonic D2-receptor activation.

Cocaine exposure produces a region-specific shift in D2-receptor sensitivity

The initial rewarding effects of cocaine are attributed to its actions in the NAc (Ikemoto and Bonci, 2014), while the later, habit-forming effects are thought to be due to actions in the DStr (Everitt and Robbins, 2013). Molecular studies have shown a variety of signaling changes downstream of both D1 and D2 receptors on MSNs (Lobo and Nestler, 2011). In addition, positron emission tomography (PET) studies have demonstrated cocaine-induced decreases in D2-receptor availability (Nader et al., 2006; Volkow et al., 2009). However, studies examining changes in D2-receptor levels following chronic cocaine exposure have been inconclusive, showing that D2-receptor density increases, decreases, or does not change (Anderson and Pierce, 2005).

As it remains unclear how cocaine administration differentially alters D2-receptor signaling in the DStr and NAc, we next sought to examine whether repeated exposure to cocaine had a region-specific effect on D2-receptor sensitivity. Mice were treated with cocaine (20 mg/kg, i.p.) for seven days and sacrificed on the eighth day (Figure 4C). Dopamine concentration-response relationships were generated for D2-receptors in the DStr and NAc medial shell of cocaine treated animals as described above (Figures 4D – 4F). Following repeated exposure to cocaine, the dopamine concentration-response curve in the DStr was unchanged with an EC_{50} of 8.8 μM ($p = 0.7$, two-way ANOVA) (Figure 4F). However, the concentration-response curve in the NAc demonstrated a rightward shift with an EC_{50} of 6.1 μM ($p < 0.001$, two-way ANOVA versus control), which was indistinguishable from DStr ($p > 0.05$, two-way ANOVA) (Figure 4F and Supplemental Table 1). This suggests that D2-receptors of the NAc medial shell had a reduced sensitivity to dopamine following chronic exposure to cocaine. In addition to changes in sensitivity, there was an increase in the ratio of phasic IPSC to total outward current generated in 3 μM dopamine in the NAc compared to control ($p < 0.05$, two-way ANOVA) (Figure 4G). This shift suggests that cocaine administration induces changes in the NAc that allow greater phasic increases in D2-receptor activation in the presence of sustained receptor activation.

D2-receptors on MSN axon collateral terminals also exhibit regional differences in sensitivity

In addition to long-range projections, MSNs make local inhibitory synaptic connections with neighboring MSNs via axon collaterals in the striatum (Chang and Kitai, 1986; Tecuapetla et al., 2009; Wilson and Groves, 1980). These GABAergic synapses are strongly modulated by dopamine and are thought to be involved in the behavioral response to cocaine (Dobbs et al., 2016; Taverna et al., 2008). As we found that D2-receptors coupling to GIRK channels exhibited differences in sensitivity for dopamine across the striatum, we next examined whether axonal receptors coupled to endogenous signaling pathways at collateral terminals also showed a similar regional difference. These experiments were done without overexpressing GIRK channels. ChR2 expression was targeted to D2-MSNs using AAV.DIO.ChR2.EYFP in A2A-Cre mice (Figure 5A). A single flash of blue light was used to excite D2-MSNs to evoke $GABA_A$-IPSCs in D1-MSNs (Figure 5B). Exogenous

dopamine inhibited $GABA_A$-IPSCs through activation of presynaptic D2-receptors on axon collateral terminals (Dobbs et al., 2016) (Figure 5C). To examine the sensitivity of D2-receptors on axon collaterals of D2-MSNs in the DStr and NAc, the inhibition of the $GABA_A$-IPSC was measured in response to different concentrations of dopamine in the presence of reuptake blocker (cocaine, 10 μM; with DHβE, 1 μM). While there was no difference in maximal inhibition, we found that axonal D2-receptors regulating collateral transmission had higher sensitivity for dopamine in the NAc than in the DStr (DStr: IC_{50} = 4.8 μM; NAc: IC_{50} = 2.1 μM, two-way ANOVA; $p < 0.05$) (Figure 5D). The concentration of dopamine required to inhibit GABA collaterals was similar to the concentration needed to evoke GIRK mediated outward currents in each region (Supplemental Table 1). The results suggest that D2-receptors on terminals of axon collaterals coupling to different signaling machinery also exhibit region-specific differences in dopamine sensitivity.

Dopamine D2/D3 receptor expression differences between the DStr and NAc do not explain regional differences in D2-receptor signaling

Dopamine D3-receptors are a D2-like receptor thought to have higher affinity for dopamine than D2-receptors (Sokoloff et al., 1990) and have higher expression levels in the NAc (Gangarossa et al., 2013). We next sought to address whether differential D3-receptor expression contributes to the regional differences in D2-receptor signaling by using the selective D3-receptor antagonist, VK4-116 (100 nM) (Kumar et al., 2016). There was no change in the amplitude or kinetics of D2-IPSCs in either the DStr or NAc ($p > 0.05$, Student's paired t-tests) (Supplemental Figures 3B and 3C). In a separate set of experiments, we injected AAV.GIRK2 in the DStr and NAc of D3-receptor knock-out (D3KO) mice and found that D2-IPSCs evoked in the DStr and NAc in D3KO mice still displayed a regional difference in kinetics ($p < 0.05$, Mann-Whitney test). There was also no difference in the maximal outward current produced by 100 μM dopamine in the presence of VK4-116 (100 nM) ($p = 0.7$, two-way ANOVA). Bath application of dopamine at a concentration near the EC_{50} for D2-receptor activation (3 μM) still produced larger currents in the NAc than in the DStr (normalized to outward current in 100 μM dopamine) in the presence of VK4-116 ($p < 0.05$, Mann-Whitney test) (Supplemental Figure 3D). Together these results show that regional differences in D2-receptor kinetics and sensitivity are preserved when D3-receptors are either genetically or pharmacologically eliminated.

We next examined how D2-receptor availability affects the kinetics of D2-IPSCs. A sub-saturating concentration of the D2-receptor antagonist sulpiride (20 nM) was used to block a fraction of D2-receptors (Supplemental Figure 3E). This concentration reduced the amplitude of D2-IPSCs in both the DStr and NAc by approximately 70% but had no effect on the kinetics of synaptic events in either region ($p > 0.05$, Student's paired t-tests) (Supplemental Figure 3F). This implies that reducing the number of available D2-receptors over this range does not alter D2-receptor signaling kinetics.

Other $Gα_{i/o}$ coupled receptors on MSNs do not display the same regional differences as D2-receptor signaling

The endogenous opioid enkephalin activates mu and delta opioid receptors on both D1-MSNs and D2-MSNs in the patch sub-compartment of the striatum (Banghart et al., 2015;

Ragsdale and Graybiel, 1981). As mu and delta opioid receptors are $G\alpha_{i/o}$ coupled, they also couple to GIRK channels when overexpressed in MSNs (Mamaligas et al., 2016a). To target opioid receptors on D2-MSNs, AAV.DIO.tdTomato.GIRK was injected into the DStr and NAc of A2A-Cre mice (Figure 6A). Whole-cell recordings were made from GIRK-expressing D2-MSNs in the presence of the peptidase inhibitors thiorphan (1 μM) and bestatin (10 μM) to prevent enkephalin degradation (Figure 6A). To examine whether opioid receptors display the same regional difference in receptor sensitivity as the D2-receptor, a leu-enkephalin concentration-response curve was generated for opioid receptor mediated GIRK currents from D2-MSNs in the DStr and NAc (Figure 6B and 6C). There was no difference in the maximum outward current produced by enkephalin (30 μM) between the DStr and NAc (p = 0.8, Mann-Whitney test). In addition, the EC_{50} of opioid receptor activation was the same in both regions (p = 0.9, two-way ANOVA) (Figure 6C and Supplemental Table 1).

We next sought to examine whether another $G\alpha_{i/o}$ coupled receptor, the M4 muscarinic receptor, on a different population of MSNs displayed the same regional difference in activation kinetics as the D2-receptor. The pacemaker firing of cholinergic interneurons and associated release of acetylcholine evokes spontaneous M4-muscarinic IPSCs in GIRK2-expressing direct pathway D1-MSNs (Mamaligas and Ford, 2016b) (Figure 6D and Supplemental Figure 4). The average amplitude of spontaneous M4-muscarinic IPSCs was the same in the DStr and NAc (p = 0.6, Mann-Whitney). In addition, spontaneous muscarinic synaptic events in DStr and NAc had similar rise and decay times (p > 0.5, Mann-Whitney tests) (Figures 6E – 6F). Thus, the mechanisms underlying the regional heterogeneity of D2-receptor activation and sensitivity are likely specific to D2-receptors and not generalizable to other $G\alpha_{i/o}$ coupled receptors on either D1-MSNs or D2-MSNs.

RGS7 and RGS9 proteins regulate the timing of synaptic events, but not D2-receptor sensitivity

D2-receptor mediated activation of GIRK channels occurs through activation of G-proteins and liberation of the Gβγ subunit, and this process can be regulated by a variety of intracellular signaling molecules. Regulator of G-protein signaling (RGS) proteins are GTPase activating proteins that regulate the timing of G-protein cycling by reducing the active lifetime of the Gα-GTP and Gβγ subunit (Anderson et al., 2009). Several RGS proteins are expressed in the striatum, including RGS9-2 and RGS7 (Thomas et al., 1998). As RGS proteins are known to regulate both the timing and sensitivity of GPCR coupling to GIRK channels in other systems (Ostrovskaya et al., 2014; Xie et al., 2010), we next sought to examine whether striatal RGS proteins could explain the observed regional differences in D2-receptor signaling kinetics and sensitivity. We crossed mice with a genetic deletion of RGS9 (Chen et al., 2000) and RGS7 (Cao et al., 2012), resulting in a mouse lacking both RGS9 and RGS7 (RGS7/9 KO).

RGS7/9 KO mice were injected with AAV.GIRK2 in the DStr and NAc medial shell (Figure 7A). Electrically evoked D2-IPSCs were similar in amplitude in RGS7/9 KO and control littermates but were slower to rise and to decay (Figures 7B – 7E). The slowing of kinetics, however, was present in both the DStr and NAc, and the different rate of D2-IPSC activation

between regions remained the same in the KO mice (10 – 90% rise: DStr = 25% increase vs. control; NAc = 22% increase vs. control; tau decay: DStr = 64% increase vs. control; NAc = 79% increase vs. control). Spontaneous M4-IPSCs recorded in D1-MSNs of both regions were also slower in RGS7/9 KO mice (Supplemental Figures 5A – 5B). In contrast to the changes in D2-receptor signaling kinetics, there was no difference in D2-receptor sensitivity between RGS7/9 KO mice and WT mice in MSNs of the DStr (p = 0.8, two-way ANOVA) (Figures 7F – 7G and Supplemental Table 1). This suggests that two members of the R7 class of RGS proteins, RGS7 and RGS9, regulate the timing but not the sensitivity of D2-receptor signaling in the striatum and that they may be one of several mechanisms controlling the rate of D2-receptor activation across regions.

G-protein coupled receptor kinases (GRKs) are another important signaling molecule that regulate GPCR signal termination. To examine the role of GRKs in regulating the timing of D2-IPSCs in the DStr and NAc, we utilized a small-molecule, membrane permeable GRK2/3 inhibitor, Compound 101 (Cpd 101, 30 μM) (Urs et al., 2016). Inhibition of GRK2/3 with Cpd 101 had no effect on IPSC amplitude in the DStr or NAc (p = 0.1, Student's paired t-tests) (Supplemental Figure 5C and 5D). Similarly, there was no change in IPSC kinetics in the presence of Cpd 101 in either region (p > 0.05; Student's paired t-tests) (Supplemental Figure 5E).

Different Gα subunit compositions in the DStr and NAc contribute to regional differences in D2-receptor sensitivity

The D2-receptor primarily couples to pertussis toxin sensitive (PTX) G protein subunits $G\alpha_i$ and $G\alpha_o$. Whereas $G\alpha_i$ is expressed similarly throughout mouse striatum, $G\alpha_o$ is enriched in the NAc (Allen Mouse Brain Atlas) (Lein et al., 2007). Previous studies in cultured cells indicate that the potency of dopamine depends on the G protein subtype to which the D2-receptor is coupled, i.e., dopamine was reported to more potently activate $G\alpha_o$ than $G\alpha_i$ based on their differential incorporation of the non-hydrolyzable GTP analog, GTPγS, upon receptor activation (Gazi et al., 2003; Lane et al., 2007). Thus, we hypothesized that although D2-receptors activate $G\alpha_i$ throughout the striatum, the greater availability of $G\alpha_o$ in the NAc results in a higher potency for dopamine in this brain region compared to the DStr.

We first confirmed that dopamine more potently activates $G\alpha_o$ than $G\alpha_i$ using a bioluminescence resonance energy transfer (BRET) based, D2-receptor dependent G protein activation assay (Newman et al., 2012), which detects agonist-induced conformational changes within defined G protein subtypes. Consistent with previous studies (Gazi et al., 2003; Lane et al., 2007), dopamine activated $G\alpha_{oA}$ with ~8-fold higher potency than $G\alpha_{i1}$ in HEK cells (n = 7 – 9; Student's two-tailed t-test, p < 0.0001) (Figure 8A). In contrast, leu-enkephalin induced MOR-dependent activation of $G\alpha_{i1}$ and $G\alpha_{oA}$ was not significantly different (n = 3; Student's two-tailed t-test, p > 0.05) (Figure 8B), indicating that the effect of dopamine on $G\alpha_i$ and $G\alpha_o$ is not simply due to inherent differences between these G proteins, but rather stems from preferential activation of $G\alpha_o$ by D2-receptors. Next, we examined whether differences in $G\alpha_i$ and $G\alpha_o$ activation by dopamine extend to GIRK channel activation. We selectively evaluated the actions of $G\alpha_i$ or $G\alpha_o$ in HEK cells by

inactivating endogenous $G\alpha_{i/o}$ with PTX and co-expressing PTX-resistant $G\alpha_{i1}$ or $G\alpha_{oA}$. Inactivating endogenous $G\alpha_{i/o}$ with pertussis toxin (PTX) abolished dopamine-induced, D2-receptor mediated GIRK1/2 activation (Supplemental Figure 6), and the co-expression of PTX-resistant $G\alpha_{i1}$ or $G\alpha_{oA}$ restored channel activation (Figure 8C). The dopamine-induced activation of GIRK1/2 was ~41-fold more potent in the presence of $G\alpha_{oA}$ compared to $G\alpha_{i1}$ (Figure 8C). Overall, these results indicate that in heterologous systems, dopamine more potently activates $G\alpha_o$ than $G\alpha_i$ downstream of D2-receptors, resulting in the higher potency activation of $G\alpha_o$-mediated signaling.

Finally, we sought to examine whether altering $G\alpha_o$ subunits in the mouse brain produced changes in D2-receptor sensitivity in the striatum. To lower $G\alpha_o$ levels, we injected an AAV encoding Cre (AAV.EF1a.Cre) into either the DStr or the NAc of $Gnao^{flx/flx}$ mice (Chamero et al., 2011) along with the AAV encoding GIRK2 (Figure 8D). In these conditional $G\alpha_o$ knockout mice ($G\alpha_o$ cKO), total striatal $G\alpha_o$ protein levels were reduced by 62% $\pm$ 7% (p < 0.01, Mann-Whitney test) (Figure 8E). The incomplete elimination of $G\alpha_o$ in the striatum is likely a result of $Gnao$ expression in other cell types not targeted by the viral vector. D2-IPSCs recorded in the DStr and NAc of $G\alpha_o$ cKO mice displayed a similar regional difference in kinetics as wildtype mice (Figure 8F). In order to determine whether deletion of $G\alpha_o$ changed the sensitivity of D2-receptor activation, we generated dopamine concentration-response curves in the DStr and NAc of $G\alpha_o$ cKO mice (Figures 8G – 8H). In the DStr, the maximum outward current was reduced following viral knockdown (one-way ANOVA with Tukey's post-test; p < 0.05 vs. control) but there was no change in the sensitivity of D2-receptor activation compared to control (cKO: EC_{50} = 7.5 μM; DStr control EC_{50} = 5.9 μM) (Figure 8H). In the NAc however, the concentration-response curve for D2-receptors in $G\alpha_o$ cKO mice was shifted to the right as compared to control, with an EC_{50} of 11.7 μM (Figure 8H and Supplemental Table 1). Thus, decreasing $G\alpha_o$ expression in the mouse brain produces a decrease in the sensitivity of D2-receptor activation specifically in the NAc. Together these results suggest that intrinsic differences in $G\alpha_o$ versus $G\alpha_i$ expression in the DStr and NAc may underlie the observed regional differences in D2-receptor sensitivity.

Discussion

Here we show that there is heterogeneity in both the timing and sensitivity of dopamine D2-receptor signaling across striatal subregions. Many of the factors regulating regional differences in striatal dopamine transmission, including dopamine transporters (Jones et al., 1995; Rice et al., 2011), presynaptic autoreceptors (Phillips et al., 2002), and nicotinic receptors (Shin et al., 2017; Threlfell et al., 2012; Zhang et al., 2009), have been previously studied using cyclic voltammetry and other electrochemical methods (Sulzer et al., 2016). While these studies have provided important insights in our understanding of striatal dopamine transmission, it has been unclear how these regional differences in dopamine release are differentially encoded by synaptic D2-receptors.

Using a synaptic readout of D2-receptor activation, we identified a previously unappreciated regional difference in D2-receptor signaling between the DStr and NAc. While decay kinetics were strongly regulated by DATs as expected (Jones et al., 1995), we found that the

activation of D2-receptors in the medial shell of the NAc occurs with intrinsically slower kinetics. This difference was not a result of differences in uptake nor in the amount of dopamine released. Using FSCV with a rapid sampling rate (100 Hz), we found that there was no difference in the rate of dopamine release between the DStr and NAc nor was the rate of release altered by blocking dopamine transporters. Furthermore, reducing the intensity of stimulation to evoke smaller D2-IPSCs in the DStr did not slow the kinetics of D2-IPSCs. This suggests that the regional difference in activation kinetics of D2-IPSCs instead was due to the intrinsic, region-specific properties of D2-receptors. In support of this, we found that local application of dopamine directly to MSN dendrites resulted in currents that activated more rapidly in the DStr than in the NAc. Using a combination of approaches in heterologous systems as well as viral mediated elimination of G-proteins, we found that a region-specific difference in D2-receptor sensitivity also exists across regions and this could be accounted for by coupling of D2-receptors to $G\alpha_o$ versus $G\alpha_i$ subunits. These results identify that multiple mechanisms shape the temporal dynamics of D2-receptor signaling across striatal regions, but sensitivity is controlled through G-protein coupling.

D2-IPSCs evoked with minimal electrical stimulation had more rapid rise kinetics than D2-receptor mediated GIRK currents evoked with focal, 2-photon guided iontophoresis. Since the activation rate of D2-receptor mediated GIRK currents is dependent on the concentration of agonist at the receptor (Courtney and Ford, 2014; Ford et al., 2009), this result suggests that a higher concentration of dopamine mediates synaptic D2-receptor activation. Postsynaptic iontophoretic GIRK currents were subject to regulation by dopamine transporters, whereas the activation rate of D2-IPSCs was independent of reuptake by transporters. This indicates that the synaptic contacts formed between dopamine terminals and MSN dendrites are likely closer than what could be approximated with 2-photon guided iontophoresis. Therefore, although striatal dopamine transmission is thought to largely occur by volume transmission and diffusion to extrasynaptic receptors (Rice et al., 2011), the activation of the synaptic currents underlying the D2-IPSC are likely mediated by receptors located near the site of release. As only a small, sparse proportion of dopamine varicosities release dopamine, but do so with rapid kinetics (Liu et al., 2018; Pereira et al., 2016), local release of dopamine at spatially defined sites may lead to the rapid activation of D2-receptors observed here. Thus, while it is well established that the magnitude of evoked dopamine release is greater in dorsal regions of the striatum (Cragg et al., 2002; Jones et al., 1995), partially as a result of more dense axonal arborization of dopamine neurons projecting to the DStr (Pacelli et al., 2015; Parent and Parent, 2006), the local concentration profile of dopamine that drives activation of receptors may be similar across regions.

Mechanisms of D2-receptor signaling

Biophysical, molecular, and pharmacological studies have shown that many factors regulate the timing and sensitivity of GPCR signaling, including the $G\alpha$ subunit, RGS proteins, receptor isoforms and heterodimers, receptor localization and trafficking, and signaling through beta arrestins (Han et al., 2009; Masuho et al., 2015; Porter-Stransky and Weinshenker, 2017). In this study, we investigated several of these key players in GPCR signaling and their role in regulating D2-receptor signaling across striatal subregions. RGS proteins accelerate the G-protein cycle by increasing the rate of GTP hydrolysis, leading to

effects on both activation and deactivation of GPCR signaling (Ross and Wilkie, 2000). Deletion of two members of the R7 class of RGS proteins, RGS7 and RGS9, in striatal MSNs led to prolongation of both the activation and decay phase of D2-IPSCs. However, since the magnitude of the change in kinetics in RGS7/9 KO mice was similar in the DStr and NAc, regional differences in RGS mediated regulation of D2-receptor signaling cannot completely explain the underlying regional kinetic differences. Previous studies have found that RGS proteins also regulate the sensitivity of GPCRs for agonist, with elimination of RGS proteins resulting in higher sensitivity signaling (Ostrovskaya et al., 2014; Xie et al., 2010). In contrast, here we found that genetic deletion of RGS7 and RGS9 did not result in increased dopamine sensitivity in the DStr. The fact that RGS7/9 KO did not produce a shift in the dose response curve in the DStr, suggests that the lower sensitivity in this region was unlikely to be due to an increased activity or expression of RGS proteins. As RGS proteins can exhibit redundancy of actions (Doupnik, 2015), it is possible that other members of the R7 class of RGS proteins can compensate for the loss of RGS7 and RGS9.

GPCRs can couple to different classes of Gα subunits with unique properties (Gazi et al., 2003; Masuho et al., 2015). By changing the composition of Gα subunits in heterologous systems, we found that dopamine more potently activates downstream signaling cascades when coupled to $G\alpha_o$ than $G\alpha_i$. We also found that viral knockdown of $G\alpha_o$ in the NAc lowered the sensitivity of dopamine. This suggests that as a result of the increased proportion of $G\alpha_o$ in the ventral striatum (Allen Mouse Brain Atlas) (Lein et al., 2007), D2-receptors couple more readily to $G\alpha_o$ in the NAc, which accounts for the increased sensitivity of D2-receptor activation in this region. The region-specific difference in D2-receptor sensitivity for dopamine was not seen across other striatal GPCRs, as there was no difference in the sensitivity of opioid receptors for leu-enkephalin between the DStr and NAc. As leu-enkephalin showed equal potency for activating $G\alpha_{oA}$ and $G\alpha_{i1}$, the agonist specific differential activation of G-proteins by D2-receptors is not shared by all GPCRs within the striatum.

Cell signaling processing can vary across neuronal domains (Castro et al., 2014), however we found that both dendritic D2-receptors coupling to GIRK channels and axonal receptors regulating collateral transmission through endogenous pathways exhibited regional differences in dopamine sensitivity. This shows that the regional differences in sensitivity are physiologically relevant to regulating striatal microcircuitry, but also suggests that the mechanism governing the regional heterogeneity is conserved across the entire arbor of the MSN. Our data suggest the possibility that the enrichment of $G\alpha_o$ in the NAc occurs at both dendritic and axonal signaling sites, leading to an increased dopamine sensitivity across the neuronal arbor.

Psychostimulant induced changes in D2-receptor signaling

Behavioral theories of cocaine addiction hold that the transition from initial to compulsive drug use corresponds with a shift in the striatal subregion controlling drug-related behaviors, from the NAc to the DStr (Everitt and Robbins, 2013). In addition to regional differences in cocaine induced behaviors, many studies have examined cell type specific alterations in striatal D1-MSN versus D2-MSN signaling in response to cocaine (Anderson and Pierce,

2005; Lobo and Nestler, 2011; Smith et al., 2013). The general consensus is that increased sensitivity to cocaine and cocaine-seeking behaviors are associated with a predominance of D1-MSN activity over D2-MSN activity (Bock et al., 2013; Lobo et al., 2010). However, studies directly examining changes in D2-receptor signaling are often confounded by the presence of D2-autoreceptors on dopamine terminals as well as D2-receptors on striatal interneurons (Kreitzer, 2009; Sulzer et al., 2016). We found that repeated exposure to cocaine produced a decrease in the sensitivity of postsynaptic D2-receptor signaling specifically in the NAc. Since dopamine reduces excitability of D2-MSNs, a decrease in D2-receptor sensitivity may serve as a compensatory response to limit D2-receptor mediated inhibition in the face of increased extracellular dopamine during cocaine use. Consistent with this, imaging studies have shown reduced D2-receptor availability in both the dorsal and ventral striatum in human addicts and non-human primates chronically treated with cocaine (Nader et al., 2006; Volkow et al., 2009). While our study utilized non-contingent cocaine administration, a similar region-specific effect of cocaine has been seen with self-administration (Bock et al., 2013), suggesting that the effect may be independent of cocaine administration paradigm. Our findings suggest that expression levels of different $G\alpha$ subunits contribute to defining dopamine sensitivity at the D2-receptor. Future studies will be required to elucidate the mechanism that underlie the shift in dopamine sensitivity following repeated exposure to cocaine as behavioral sensitization to cocaine is not associated with changes in G-protein levels (Perrine et al., 2005).

In conclusion, we show here that not all D2-receptor signaling is inherently the same but differs as a result of unique complements of signaling partners in different populations of MSNs. This allows for fine-tuning of D2-receptor signaling across striatal subregions at the level of the postsynaptic membrane. These regional differences in signaling produce physiologically relevant changes in how D2-receptors encode different dopamine release events in nigrostriatal and mesolimbic circuits.

STAR Methods

Experimental Model and Subject Details. Stereotaxic injections

All animal procedures were performed in accordance with the guidelines of the Institutional Animal Care and Use Committee (IACUC) at the University of Colorado School of Medicine and Case Western Reserve University. Transgenic mice utilized in experiments were dopamine transporter (DAT) IRES Cre heterozygote mice (The Jackson Laboratory), Adora2a (A2A)-Cre heterozygote mice (GENSAT), Drd1-Cre heterozygote mice (The Jackson Laboratory), DAT-knockout mice (Giros et al., 1996), Drd3-knockout mice, and $G\alpha_o$ fl/fl mice (Charles River, Chamero et al., 2011), RGS9 KO (Chen et al., 2000), RGS7 KO (Cao et al., 2012) as indicated in the body of the text. Mice underwent stereotaxic injections at postnatal day 21. Both male and female juvenile/young adult mice (3–8 weeks) were used throughout the study. Adenoassociated virus (AAV) was injected with a pulled pipette using a Nanoject II (Drummond Scientific). All AAVs were from the University of Pennsylvania Viral Core or the University of North Carolina Viral Core. For experiments with ChR2, 500 nL AAV5.EF1a. DIO.hChR2(H134R)-EYFP.WPRE.hGH was injected into either the midbrain (SNc and VTA) of DAT-Cre mice, or the striatum (DStr or NAc) of

A2A-Cre mice (GABA collateral experiments). Coordinates for midbrain injections were: AP − 2.3 mm, ML + 0.45 mm, − 4.7 mm. Coordinates for DStr injections were AP + 1.2 mm, ML + 1.8 mm, − 3.35 mm and NAc injections were AP + 1.4 mm, ML + 1.25 mm, − 4.15 mm. For striatal injections, 300 nL of AAV2/9.hSynapsin.tdTomato.T2A.mGIRK2-1-A22A.WPRE was injected into the DStr and the NAc. For cell-type specific experiments, AAV9.hSynapsin.DIO.tdTomato.T2A.mGIRK2-1-A22A.WPRE was injected into the DStr and NAc of A2A-Cre or D1-Cre mice. There was no difference between electrically evoked D2-IPSCs recorded in GIRK2$^+$ MSNs from DAT-Cre mice and A2A-Cre mice. For experiments in Gα_o fl/fl mice, AAV5.EF1a.Cre was mixed with AAV2/9.hSynapsin.tdTomato.T2A.mGIRK2-1-A22A.WPRE and injected into the DStr or NAc. Animals recovered for at least 4.5 weeks following surgery.

Slice preparation

Coronal brain slices (240 μM) containing the DStr and NAc were cut in ice-cold physiological saline solution containing (in mM) 75 NaCl, 2.5 KCl, 6 MgCl$_2$, 0.1 CaCl$_2$, 1.2 NaH$_2$PO$_4$, 25 NaHCO$_3$, 2.5 D-glucose and 50 sucrose. Slices were incubated at 32 °C for at least 45 minutes and bubbled constantly with 95% O$_2$ and 5% CO$_2$ in ASCF containing (in mM) 126 NaCl, 2.5 KCl, 1.2 MgCl$_2$, 2.5 CaCl$_2$, 1.2 NaH$_2$PO$_4$, 21.4 NaHCO$_3$, 11.1 D-glucose and 10 μM MK-801 to prevent excitotoxicity. Following incubation, slices were transferred to the recording chamber and constantly perfused (2 mL/min) with ACSF (33 ± 2 °C). ACSF used for recording contained picrotoxin (100 μM), SCH 23390 (1 μM), scopolamine (200 nM), and CGP 55845 (300 nM). Dihydro-β-erythroidine hydrobromide (DHβE, 1 μM) was included in the recording solution where indicated in the text. A BXWI51 microscope (Olympus) was used to visualize MSNs with infrared gradient contrast optics. Fluorescence from tdTomato was visualized with an LED (Thorlabs).

Electrophysiology

Whole-cell voltage clamp recordings (V$_h$ = −60 mV) were made from tdTomato$^+$ (GIRK2$^+$) MSNs using Axopatch 200B amplifiers (Molecular Devices) and acquired with Axograph X (Axograph Scientific) at 5 kHz and filtered to 2 kHz. Patch pipettes (1.5 – 2 MΩ) (World Precision Instruments) contained 115 mM K-methylsulphate, 20 mM NaCl, 1.5 mM MgCl$_2$, 10 mM HEPES(K), 10 mM BAPTA-tetrapotassium, 1 mg/mL ATP, 0.1 mg/mL GTP, and 1.5 mg/mL phosphocreatine (pH 7.4, 275 mOsm). No series resistance compensation was used and cells were discarded if series resistance increased above 15 MΩ.

Optogenetic stimulation of dopamine release was elicited using wide-field blue light (pulse width = 2 ms, ~1 mW) through the objective from a blue LED (470nm, Thorlabs or Luxeon Star LEDs). About half of GIRK2$^+$ MSNs recorded displayed D2-IPSCs in response to optogenetic stimulation, identifying them as D2-MSNs (Marcott et al., 2014). For D2-IPSC recordings, DNQX was excluded in some cases to measure AMPA-EPSCs resulting from glutamate release from dopamine terminals. Addition of DNQX (10 μM) to block EPSCs did not affect D2-IPSCs. For M4-IPSC recordings in D1-MSNs, scopolamine was omitted from the recording solution and spontaneous events were detected using Axograph X (Axograph Scientific). For recordings of leu-enkephalin mediated GIRK currents, thiorphan (1 μM) and bestatin (10 μM) were included in the recording solution to inhibit degradation.

Where indicated, electrical stimulation was used to evoke dopamine release using a monopolar glass stimulating electrode filled with ACSF. DHβE (1 μM) was always included in the recording solution in experiments using electrical stimulation to block cholinergic interneuron mediated activation of dopamine terminals (Mamaligas et al., 2016b). For dopamine bath application experiments, cocaine (10 μM; with DHβE, 1 μM) was included in the recording solution to block reuptake and allow equal penetration of dopamine into the slice in the DStr and NAc. Drugs were applied by bath perfusion. For high and low optogenetic stimulation, optical stimulation intensity was reduced by approximately half from a high values of ~1 mw.

For GABA collateral recordings in A2A-Cre mice, the internal solution contained 135 mM CsCl, 0.1 mM CaCl$_2$, 2 mM MgCl$_2$, 10 mM HEPES(K), 0.1 mM EGTA, 1 mg/mL ATP, 0.1 mg/mL GTP, 1.5 mg/mL phosphocreatine, and 3.3 mM QX-314 (Cl$^-$ salt) (pH 7.4, 275 mOsm). Whole-cell recordings (V$_h$ = −60 mV) were made from putative D1-MSNs and GABA release from ChR2-expressing D2-MSNs was evoked with wide-field blue light (pulse width = 1 ms) every 30 seconds. Recording solution contained SCH 23390 (1 μM), scopolamine (200 nM), DNQX (10 μM), CGP 55845 (300 nM), DHβE (1 μM), and cocaine (10 μM). GABA$_A$-IPSCs recorded 5 minutes prior to dopamine bath application were used for baseline. Recordings were filtered to 5 kHz.

2-photon imaging

Fluorescent imaging was performed using a BX51WI (Olympus) microscope and a home-built 2-photon laser scanning microscopy system using a pair of XY galvanometer mirrors (6215, Cambridge Technology) using custom imaging software. A Mira 900 Ti:sapphire laser with a Verdi G10 pump laser (Coherent) was tuned to 800 nm and epifluorescence signals were captured through a 60× water immersion objective (Olympus) using a T700LPXXR dichroic mirror and ET680sp and ET620/60 filters (Chroma) and a H10721-20 photomultiplier tube (Hamamatsu). A SR570 current preamplifier (Stanford Research Systems) was used to convert the output to voltage and the signal was digitized using a NI PCI-6110 data acquisition board (National Instruments). Bidirectional waveforms were generated using custom code in Visual Studio and Python. MSNs were visualized by including Alexa 594 (20 μM) in the patch pipette. Internal solution for 2-photon experiments also included 135 mM D-gluconate(K), 10 mM HEPES(K), 0.1 mM CaCl$_2$, 2 mM MgCl$_2$, 0.1 mM EGTA, 1 mg/mL ATP, 0.1 mg/mL GTP, and 1.5 mg/mL phosphocreatine (pH 7.4, 275 mOsm). For dopamine iontophoresis, a thin-walled glass iontophoretic electrode was filled with dopamine (1 M) including sulforhodamine 101 (300 μM) and was briefly dipped for ~ 30 s in a solution containing BSA-conjugated Alexa 594 (0.06 %). Dopamine was ejected as a cation (160 nA) in 2 – 5 ms pulses for minimum iontophoresis. Leakage of dopamine was prevented with a retention current of 3 – 20 nA.

FSCV

Carbon fiber electrodes (34 – 700, Goodfellow) were encased with a glass pipette with an exposed diameter of 7 μm and length of 50 – 100 μm. The tip of the carbon fiber was soaked in activated carbon-purified isopropanol for at least 20 – 30 minutes before using. The tip of fiber was placed in the DStr or NAc medial shell 30 – 70 μm below the surface of the slice.

While holding the carbon fiber at –0.4 V, triangular waveforms (–0.4 to 1.3 V versus Ag/AgCl at 400 V/s) were applied to the fiber at 10 Hz. Background subtracted cyclic voltammogram currents were obtained by subtracting the average of 10 voltammograms obtained prior to stimulation from each voltammogram obtained after stimulation. The time course of dopamine transmission was determined by plotting the peak oxidation potential versus time. The carbon fiber was calibrated to known concentrations of dopamine after experiments. For kinetic FSCV experiments, triangular waveforms (–0.4 to 1.0 V versus Ag/AgCl at 600 V/s) were applied to the fiber at 100 Hz. LED flash hitting the carbon fiber resulted in a photovoltaic artifact that obscured the rise phase of release. At the end of experiments, tetrodotoxin (TTX, 200 nM) was applied to the slice to eliminate all action potential dependent release and isolate the artifact, which was then subtracted from FSCV transients to allow for analysis of the kinetics of dopamine release. Optogenetic stimulation parameters were the same as those used for electrophysiology. DHβE (1 μM) was always included in the recording solution for FSCV experiments.

Western Blots

The striatum for western analysis was isolated and performed as previously described (Marcott et al., 2014). The samples were denatured with STE buffer (10 mM Tris-Cl, pH 7.5, 1 mM EDTA, pH 8.0, 10% SDS) at 100 °C for 5 min and equivalent amounts of protein were subjected to SDS-PAGE on 10% polyacrylamide gels, and then transferred to methanol activated PVDF membrane (Perkin Elmer). Blots were blocked by 5% milk for 1 hour at RT and then incubated with primary antibody against Gαo protein (1:500, Santa Cruz, sc-13532) at 4°C over night. Following incubation with horseradish peroxidase (HRP)-conjugated secondary antibody for 1 hour at 37°C, blots were incubated in Pierce ECL reagent (ThermoFisher) and visualized with a Cheimager (Alpha Innotech). The densitometry was quantified with ImageJ.

Molecular biology and heterologous expression

All constructs used in the cell-based assays were cloned into the pcDNA3.1 vector. For the bioluminescence resonance energy transfer (BRET)-based assays, HEK293T cells were seeded onto 10 cm plates and transfected with a 1:1 ratio of DNA:polyethylenimine (linear, MW 25,000; PolySciences, Inc.). For the BRET-based receptor-mediated G_{i1} and G_{oA} activation assays, cells were transfected with plasmids encoding hD2s (0.2 μg) or mMORs (0.2 μg), and $G\beta_1$ and $G\gamma_2$ fused to the split mVenus fragments V1 and V2, respectively (V1-Gβ_1 (1 μg) and V2-Gγ_2 (7 μg)), as well as PTX-resistant $G\alpha_{i1}$ or $G\alpha_{oA}$ with *Renilla* luciferase 8 (Rluc8) inserted at amino acid position 91 ($G\alpha_{i1}$-91-Rluc8 (0.2 μg) or $G\alpha_{oA}$-91-Rluc8 (0.1 μg)). For the cell-based GIRK assay, HEK293T cells were sparsely seeded onto 18 mm coverslips and were transiently transfected with plasmids encoding hD2s (0.1 μg), PTX-resistant $G\alpha_{i1}$ or $G\alpha_{oA}$ (0.1 μg), human GIRK1 (0.7 μg), human GIRK2 (0.7 μg), the S1 catalytic subunit of PTX (S1-PTX; 0.1 μg) and tdTomato (0.7 μg) with Lipofectamine 2000 (Invitrogen).

Bioluminescence resonance energy transfer (BRET) assays

All BRET studies were performed in HEK293T cells that were maintained in DMEM (Invitrogen) with 10% fetal bovine serum at 37 °C under 5% CO_2. Cells were transiently

transfected with the plasmids described above. Cells were prepared and assayed as described previously in detail (Donthamsetti et al., 2015; Newman et al., 2012). Briefly, cells were washed, harvested and resuspended in DPBS containing 5 mM glucose at room temperature. Cells (~40 μg of protein per well according to a BCA protein assay kit, ThermoScientific) were distributed into a 96-well microplate (Wallac, PerkinElmer Life and Analytical Sciences). After incubation with coelenterazine H (5 μM) (Dalton Pharma Services) for 8 minutes, different ligands were injected and incubated for 2 to 10 minutes. Using a Pherastar FS plate reader (BMG Labtech), BRET signal was determined by quantifying and calculating the ratio of the light emitted by mVenus (510–540 nm) over that emitted by Rluc8 (485 nm).

GIRK activation assay in cultured cells

HEK293T cells were maintained in DMEM (Invitrogen) with 10% fetal bovine serum on poly-L-lysine-coated coverslips. Cells were patch-clamped in whole-cell configuration 16–24 hours after transfection in high potassium solution containing 120 mM KCl, 25 mM NaCl, 10 mM HEPES, 2 mM $CaCl_2$ and 1 mM $MgCl_2$, pH 7.4. Glass pipettes with a resistance of 3–7 MΩ were filled with intracellular solution containing 140 mM KCl, 10 mM HEPES, 3 mM Na_2ATP, 0.2 mM Na_2GTP, 5 mM EGTA and 3 mM $MgCl_2$, pH 7.4. Cells were voltage clamped to −60 or −80 mV using an Axopatch 200A (Molecular Devices) amplifier. All pharmacological compounds were applied using a gravity-driven perfusion system.

Statistics

Statistical analyses were performed in Prism 7 (GraphPad). Data are shown as mean ± SEM. Statistical significance was defined as p 0.05 (ns), $p < 0.05$ (*), $p < 0.01$ (**), and $p < 0.001$ (***). Statistical significance was determined using Mann-Whitney U test, Student's paired t-test, Wilcoxon signed-rank test, and two-way ANOVA, as appropriate, with Tukey's post hoc analysis. Onset of D2-IPSCs was measured as time to two S.D. above noise. The EC_{50}/IC_{50} of D2-receptor activation in each area was calculated by fitting data points using nonlinear regression (Hill coefficient = 1). If the maximum response and inhibition did not differ between regions, the concentration-response curves were constrained to the average maximum values measured in the two regions. Data collected in heterologous experiments were analyzed using GraphPad Prism, Clampfit (Axon instruments) or Origin (OriginLab) software. For dose-response curves, data were normalized to vehicle (0%) and dopamine (100%) and nonlinear regression analysis was performed using the sigmoidal dose–response function in GraphPad Prism.

Reagents

Picrotoxin, MK-801, SCH 23390, CGP 55845, scopolamine hydrobromide, nomifensine maleate, DHBE, enkephalin, and DHβE were from Tocris Bioscience. K-methylsulphate was from Acros Organic, and BAPTA was from Invitrogen. Vk4-116 was synthesized by Anver Shaik at NIH NIDA (Supplemental Figure 3). Cocaine hydrochloride was obtained from the National Institute of Drug Abuse. Dopamine hydrochloride and D-gluconate(K) were from Sigma-Aldrich. All other chemicals were from Fisher Scientific.

Supplementary Material

Refer to Web version on PubMed Central for supplementary material.

Acknowledgments

References

Anderson SM, Pierce RC. Cocaine-induced alterations in dopamine receptor signaling: implications for reinforcement and reinstatement. Pharmacol Ther. 2005; 106:389–403. [PubMed: 15922019]

Anderson GR, Lujan R, Martemyanov KA. Changes in striatal signaling induce remodeling of RGS complexes containing Gbeta5 and R7BP subunits. Mol Cell Biol. 2009; 29:3033–3044. [PubMed: 19332565]

Banghart MR, Neufeld SQ, Wong NC, Sabatini BL. Enkephalin Disinhibits Mu Opioid Receptor-Rich Striatal Patches via Delta Opioid Receptors. Neuron. 2015; 88:1227–1239. [PubMed: 26671460]

Bock R, Shin JH, Kaplan AR, Dobi A, Markey E, Kramer PF, Gremel CM, Christensen CH, Adrover MF, Alvarez VA. Strengthening the accumbal indirect pathway promotes resilience to compulsive cocaine use. Nat Neurosci. 2013; 16:632–638. [PubMed: 23542690]

Cao Y, Pahlberg J, Sarria I, Kamasawa N, Sampath AP, Martemyanov KA. Regulators of G protein signaling RGS7 and RGS11 determine the onset of the light response in ON bipolar neurons. Proc Natl Acad Sci U S A. 2012; 109:7905–7910. [PubMed: 22547806]

Castro LRV, Guiot E, Polito M, Paupardin-Tritsch D, Vincent P. Decoding spatial and temporal features of neuronal cAMP/PKA signaling with FRET biosensors. Biotechnol J. 2014; 9:192–202. [PubMed: 24478276]

Chamero P, Katsoulidou V, Hendrix P, Bufe B, Roberts R, Matsunami H, Abramowitz J, Birnbaumer L, Zufall F, Leinders-Zufall T. G protein G(alpha)o is essential for vomeronasal function and aggressive behavior in mice. Proc Natl Acad Sci U S A. 2011; 108:12898–12903. [PubMed: 21768373]

Chang HT, Kitai ST. Intracellular recordings from rat nucleus accumbens neurons in vitro. Brain Res. 1986; 366:392–396. [PubMed: 3008914]

Chen CK, Burns ME, He W, Wensel TG, Baylor DA, Simon MI. Slowed recovery of rod photoresponse in mice lacking the GTPase accelerating protein RGS9-1. Nature. 2000; 403:557–560. [PubMed: 10676965]

Courtney NA, Ford CP. The timing of dopamine- and noradrenaline-mediated transmission reflects underlying differences in the extent of spillover and pooling. J Neurosci Off J Soc Neurosci. 2014; 34:7645–7656.

Cragg SJ, Hille CJ, Greenfield SA. Functional domains in dorsal striatum of the nonhuman primate are defined by the dynamic behavior of dopamine. J Neurosci Off J Soc Neurosci. 2002; 22:5705–5712.

Di Chiara G, Imperato A. Drugs abused by humans preferentially increase synaptic dopamine concentrations in the mesolimbic system of freely moving rats. Proc Natl Acad Sci U S A. 1988; 85:5274–5278. [PubMed: 2899326]

Dobbs LK, Kaplan AR, Lemos JC, Matsui A, Rubinstein M, Alvarez VA. Dopamine Regulation of Lateral Inhibition between Striatal Neurons Gates the Stimulant Actions of Cocaine. Neuron. 2016; 90:1100–1113. [PubMed: 27181061]

Donthamsetti P, Quejada JR, Javitch JA, Gurevich VV, Lambert NA. Using Bioluminescence Resonance Energy Transfer (BRET) to Characterize Agonist-Induced Arrestin Recruitment to

Modified and Unmodified G Protein-Coupled Receptors. Curr Protoc Pharmacol. 2015; 70:2.14.1–14. [PubMed: 26331887]

Doupnik CA. RGS Redundancy and Implications in GPCR-GIRK Signaling. Int Rev Neurobiol. 2015; 123:87–116. [PubMed: 26422983]

Everitt BJ, Robbins TW. From the ventral to the dorsal striatum: devolving views of their roles in drug addiction. Neurosci Biobehav Rev. 2013; 37:1946–1954. [PubMed: 23438892]

Ewing AG, Bigelow JC, Wightman RM. Direct in vivo monitoring of dopamine released from two striatal compartments in the rat. Science. 1983; 221:169–171. [PubMed: 6857277]

Ford CP, Phillips PEM, Williams JT. The Time Course of Dopamine Transmission in the Ventral Tegmental Area. J Neurosci. 2009; 29:13344–13352. [PubMed: 19846722]

Gangarossa G, Espallergues J, de Kerchove d'Exaerde A, El Mestikawy S, Gerfen CR, Hervé D, Girault J-A, Valjent E. Distribution and compartmental organization of GABAergic medium-sized spiny neurons in the mouse nucleus accumbens. Front Neural Circuits. 2013; 7

Garris PA, Wightman RM. Different kinetics govern dopaminergic transmission in the amygdala, prefrontal cortex, and striatum: an in vivo voltammetric study. J Neurosci Off J Soc Neurosci. 1994; 14:442–450.

Gazi L, Nickolls SA, Strange PG. Functional coupling of the human dopamine D2 receptor with G alpha i1, G alpha i2, G alpha i3 and G alpha o G proteins: evidence for agonist regulation of G protein selectivity. Br J Pharmacol. 2003; 138:775–786. [PubMed: 12642378]

Gerfen CR, Surmeier DJ. Modulation of striatal projection systems by dopamine. Annu Rev Neurosci. 2011; 34:441–466. [PubMed: 21469956]

Giros B, Jaber M, Jones SR, Wightman RM, Caron MG. Hyperlocomotion and indifference to cocaine and amphetamine in mice lacking the dopamine transporter. Nature. 1996; 379:606–612. [PubMed: 8628395]

Graham DL, Hoppenot R, Hendryx A, Self DW. Differential ability of D1 and D2 dopamine receptor agonists to induce and modulate expression and reinstatement of cocaine place preference in rats. Psychopharmacology (Berl). 2007; 191:719–730. [PubMed: 16835769]

Haber SN, Fudge JL, McFarland NR. Striatonigrostriatal Pathways in Primates Form an Ascending Spiral from the Shell to the Dorsolateral Striatum. J Neurosci. 2000; 20:2369–2382. [PubMed: 10704511]

Han Y, Moreira IS, Urizar E, Weinstein H, Javitch JA. Allosteric communication between protomers of dopamine class A GPCR dimers modulates activation. Nat Chem Biol. 2009; 5:688–695. [PubMed: 19648932]

Ikemoto S, Bonci A. Neurocircuitry of drug reward. Neuropharmacology. 2014; 76(Pt B):329–341. [PubMed: 23664810]

Jones SR, Garris PA, Kilts CD, Wightman RM. Comparison of dopamine uptake in the basolateral amygdaloid nucleus, caudate-putamen, and nucleus accumbens of the rat. J Neurochem. 1995; 64:2581–2589. [PubMed: 7760038]

Kreitzer AC. Physiology and Pharmacology of Striatal Neurons. Annu Rev Neurosci. 2009; 32:127–147. [PubMed: 19400717]

Kumar V, Bonifazi A, Ellenberger MP, Keck TM, Pommier E, Rais R, Slusher BS, Gardner E, You Z-B, Xi Z-X, et al. Highly Selective Dopamine D3 Receptor (D3R) Antagonists and Partial Agonists Based on Eticlopride and the D3R Crystal Structure: New Leads for Opioid Dependence Treatment. J Med Chem. 2016; 59:7634–7650. [PubMed: 27508895]

Lane JR, Powney B, Wise A, Rees S, Milligan G. Protean agonism at the dopamine D2 receptor: (S)-3-(3-hydroxyphenyl)-N-propylpiperidine is an agonist for activation of Go1 but an antagonist/inverse agonist for Gi1,Gi2, and Gi3. Mol Pharmacol. 2007; 71:1349–1359. [PubMed: 17287401]

Lein ES, Hawrylycz MJ, Ao N, Ayres M, Bensinger A, Bernard A, Boe AF, Boguski MS, Brockway KS, Byrnes EJ, et al. Genome-wide atlas of gene expression in the adult mouse brain. Nature. 2007; 445:168–176. [PubMed: 17151600]

Liu C, Kershberg L, Wang J, Schneeberger S, Kaeser PS. Dopamine Secretion Is Mediated by Sparse Active Zone-like Release Sites. Cell. 2018; 172:706–718. e15. [PubMed: 29398114]

Lobo MK, Nestler EJ. The striatal balancing act in drug addiction: distinct roles of direct and indirect pathway medium spiny neurons. Front Neuroanat. 2011; 5:41. [PubMed: 21811439]

Lobo MK, Covington HE, Chaudhury D, Friedman AK, Sun H, Damez-Werno D, Dietz DM, Zaman S, Koo JW, Kennedy PJ, et al. Cell type-specific loss of BDNF signaling mimics optogenetic control of cocaine reward. Science. 2010; 330:385–390. [PubMed: 20947769]

Lowe JD, Sanderson HS, Cooke AE, Ostovar M, Tsisanova E, Withey SL, Chavkin C, Husbands SM, Kelly E, Henderson G, et al. Role of G Protein-Coupled Receptor Kinases 2 and 3 in μ-Opioid Receptor Desensitization and Internalization. Mol Pharmacol. 2015; 88:347–356. [PubMed: 26013542]

Mamaligas AA, Cai Y, Ford CP. Nicotinic and opioid receptor regulation of striatal dopamine D2-receptor mediated transmission. Sci Rep. 2016a; 6:37834. [PubMed: 27886263]

Mamaligas AA, Ford CP. Spontaneous Synaptic Activation of Muscarinic Receptors by Striatal Cholinergic Neuron Firing. Neuron. 2016b; 91:574–586. [PubMed: 27373830]

Marcott PF, Mamaligas AA, Ford CP. Phasic Dopamine Release Drives Rapid Activation of Striatal D2-Receptors. Neuron. 2014; 84:164–176. [PubMed: 25242218]

Marshall JF, O'Dell SJ, Navarrete R, Rosenstein AJ. Dopamine high-affinity transport site topography in rat brain: Major differences between dorsal and ventral striatum. Neuroscience. 1990; 37:11–21. [PubMed: 2243588]

Masuho I, Ostrovskaya O, Kramer GM, Jones CD, Xie K, Martemyanov KA. Distinct profiles of functional discrimination among G proteins determine the actions of G protein–coupled receptors. Sci Signal. 2015; 8:ra123–ra123. [PubMed: 26628681]

Nader MA, Morgan D, Gage HD, Nader SH, Calhoun TL, Buchheimer N, Ehrenkaufer R, Mach RH. PET imaging of dopamine D2 receptors during chronic cocaine self-administration in monkeys. Nat Neurosci. 2006; 9:1050–1056. [PubMed: 16829955]

Newman AH, Beuming T, Banala AK, Donthamsetti P, Pongetti K, LaBounty A, Levy B, Cao J, Michino M, Luedtke RR, et al. Molecular determinants of selectivity and efficacy at the dopamine D3 receptor. J Med Chem. 2012; 55:6689–6699. [PubMed: 22632094]

Ostrovskaya O, Xie K, Masuho I, Fajardo-Serrano A, Lujan R, Wickman K, Martemyanov KA. RGS7/Gβ5/R7BP complex regulates synaptic plasticity and memory by modulating hippocampal GABABR-GIRK signaling. ELife. 2014; 3:e02053. [PubMed: 24755289]

Pacelli C, Giguère N, Bourque MJ, Lévesque M, Slack RS, Trudeau L-É. Elevated Mitochondrial Bioenergetics and Axonal Arborization Size Are Key Contributors to the Vulnerability of Dopamine Neurons. Curr Biol CB. 2015; 25:2349–2360. [PubMed: 26320949]

Parent M, Parent A. Relationship between axonal collateralization and neuronal degeneration in basal ganglia. J Neural Transm. 2006; (Suppl):85–88.

Park K, Volkow ND, Pan Y, Du C. Chronic Cocaine Dampens Dopamine Signaling during Cocaine Intoxication and Unbalances D1 over D2 Receptor Signaling. J Neurosci. 2013; 33:15827–15836. [PubMed: 24089490]

Pereira DB, Schmitz Y, Mészáros J, Merchant P, Hu G, Li S, Henke A, Lizardi-Ortiz JE, Karpowicz RJ Jr, Morgenstern TJ, et al. Fluorescent false neurotransmitter reveals functionally silent dopamine vesicle clusters in the striatum. Nat Neurosci. 2016; 19:578–586. [PubMed: 26900925]

Perrine SA, Schroeder JA, Unterwald EM. Behavioral sensitization to binge-pattern cocaine administration is not associated with changes in protein levels of four major G-proteins. Brain Res Mol Brain Res. 2005; 133:224–232. [PubMed: 15710239]

Phillips PEM, Hancock PJ, Stamford JA. Time window of autoreceptor-mediated inhibition of limbic and striatal dopamine release. Synap N Y N. 2002; 44:15–22.

Phillips PEM, Stuber GD, Heien MLAV, Wightman RM, Carelli RM. Subsecond dopamine release promotes cocaine seeking. Nature. 2003; 422:614–618. [PubMed: 12687000]

Porter-Stransky KA, Weinshenker D. Arresting the Development of Addiction: The Role of β-Arrestin2 in Drug Abuse. J Pharmacol Exp Ther. 2017; 361:41–348.

Ragsdale CW, Graybiel AM. The fronto-striatal projection in the cat and monkey and its relationship to inhomogeneities established by acetylcholinesterase histochemistry. Brain Res. 1981; 208:259–266. [PubMed: 6163506]

Rice ME, Patel JC, Cragg SJ. Dopamine release in the basal ganglia. Neuroscience. 2011; 198:112–137. [PubMed: 21939738]

Ross EM, Wilkie TM. GTPase-activating proteins for heterotrimeric G proteins: regulators of G protein signaling (RGS) and RGS-like proteins. Annu Rev Biochem. 2000; 69:795–827. [PubMed: 10966476]

Self DW. Dopamine Receptor Subtypes in Reward and Relapse. In: Neve KA, editorThe Dopamine Receptors New York, NY: Humana Press; 2010 479523

Shin JH, Adrover MF, Alvarez VA. Distinctive modulation of dopamine release in the nucleus accumbens shell mediated by dopamine and acetylcholine receptors. J Neurosci. 2017 0596-17.

Smith RJ, Lobo MK, Spencer S, Kalivas PW. Cocaine-induced adaptations in D1 and D2 accumbens projection neurons (a dichotomy not necessarily synonymous with direct and indirect pathways). Curr Opin Neurobiol. 2013; 23:546–552. [PubMed: 23428656]

Sokoloff P, Giros B, Martres MP, Bouthenet ML, Schwartz JC. Molecular cloning and characterization of a novel dopamine receptor (D3) as a target for neuroleptics. Nature. 1990; 347:146–151. [PubMed: 1975644]

Stamford JA, Kruk ZL, Palij P, Millar J. Diffusion and uptake of dopamine in rat caudate and nucleus accumbens compared using fast cyclic voltammetry. Brain Res. 1988; 448:381–385. [PubMed: 3378163]

Sulzer D, Cragg SJ, Rice ME. Striatal dopamine neurotransmission: regulation of release and uptake. Basal Ganglia. 2016; 6:123–148. [PubMed: 27141430]

Taverna S, Ilijic E, Surmeier DJ. Recurrent Collateral Connections of Striatal Medium Spiny Neurons Are Disrupted in Models of Parkinson's Disease. J Neurosci. 2008; 28:5504–5512. [PubMed: 18495884]

Tecuapetla F, Koós T, Tepper JM, Kabbani N, Yeckel MF. Differential Dopaminergic Modulation of Neostriatal Synaptic Connections of Striatopallidal Axon Collaterals. J Neurosci. 2009; 29:8977–8990. [PubMed: 19605635]

Thomas EA, Danielson PE, Sutcliffe JG. RGS9: a regulator of G-protein signalling with specific expression in rat and mouse striatum. J Neurosci Res. 1998; 52:118–124. [PubMed: 9556034]

Threlfell S, Lalic T, Platt NJ, Jennings KA, Deisseroth K, Cragg SJ. Striatal Dopamine Release Is Triggered by Synchronized Activity in Cholinergic Interneurons. Neuron. 2012; 75:58–64. [PubMed: 22794260]

Urs NM, Gee SM, Pack TF, McCorvy JD, Evron T, Snyder JC, Yang X, Rodriguiz RM, Borrelli E, Wetsel WC, et al. Distinct cortical and striatal actions of a β-arrestin–biased dopamine D2 receptor ligand reveal unique antipsychotic-like properties. Proc Natl Acad Sci. 2016; 113:E8178–E8186. [PubMed: 27911814]

Volkow ND, Fowler JS, Wang GJ, Baler R, Telang F. Imaging dopamine's role in drug abuse and addiction. Neuropharmacology. 2009; 56(Suppl 1):3–8. [PubMed: 18617195]

Willuhn I, Wanat MJ, Clark JJ, Phillips PEM. Dopamine signaling in the nucleus accumbens of animals self-administering drugs of abuse. Curr Top Behav Neurosci. 2010; 3:29–71. [PubMed: 21161749]

Wilson CJ, Groves PM. Fine structure and synaptic connections of the common spiny neuron of the rat neostriatum: a study employing intracellular inject of horseradish peroxidase. J Comp Neurol. 1980; 194:599–615. [PubMed: 7451684]

Xie K, Martemyanov KA. Control of striatal signaling by g protein regulators. Front Neuroanat. 2011; 5:49. [PubMed: 21852966]

Xie K, Allen KL, Kourrich S, Colón-Saez J, Thomas MJ, Wickman K, Martemyanov KA. Gbeta5 recruits R7 RGS proteins to GIRK channels to regulate the timing of neuronal inhibitory signaling. Nat Neurosci. 2010; 13:661–663. [PubMed: 20453851]

Xie K, Masuho I, Brand C, Dessauer CW, Martemyanov KA. The complex of G protein regulator RGS9-2 and Gβ(5) controls sensitization and signaling kinetics of type 5 adenylyl cyclase in the striatum. Sci Signal. 2012; 5:ra63. [PubMed: 22932702]

Zhang L, Doyon WM, Clark JJ, Phillips PEM, Dani JA. Controls of tonic and phasic dopamine transmission in the dorsal and ventral striatum. Mol Pharmacol. 2009; 76:396–404. [PubMed: 19460877]

Highlights

- D2R sensitivity and rate of activation differ between dorsal and ventral striatum

- Differences occur at the level of D2R signaling throughout MSN arbor

- Differences are specific for D2Rs and not seen for other GPCRs

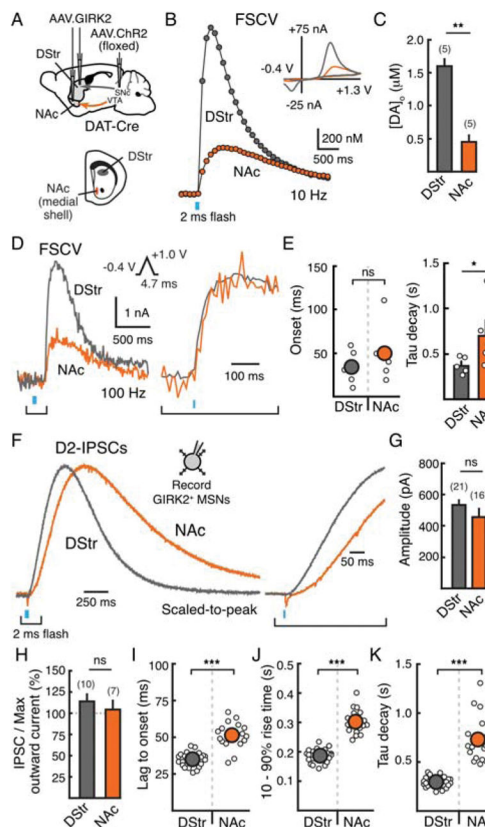- Chronic cocaine exposure selectively reduces NAc D2R sensitivity

Figure 1. D2-receptor mediated GIRK currents are faster in DStr than NAc medial shell

A) Top: Injection schematic of AAV.hSyn.tdTomato.GIRK2 into the DStr and NAc and AAV.DIO.ChR2 into the midbrain of DAT-IRES-Cre mice. Bottom: Cartoon schematic of a coronal brain slice depicting the DStr (gray) and NAc medial shell (orange).

B) Average FSCV traces (10 Hz) measuring $[DA]_o$ in the DStr and NAc medial shell in response to optogenetic stimulation of dopamine terminals (2 ms pulse, 470 nm, ~1.0 mW). Inset: cyclic voltammograms from both regions.

C) Peak $[DA]_o$ measured by FSCV in the DStr and NAc following optogenetic stimulation.

D) Average FSCV traces (100 Hz) in the DStr and NAc in response to optogenetic stimulation. Inset: FSCV waveform for kinetic experiments, scaled-to-peak magnification of rise phase.

E) Quantification of the lag to onset (time to reach two s.d. above noise) and tau of decay of FSCV transients (100 Hz).

F) Representative traces of optogenetically evoked D2-IPSCs from the DStr and NAc. Inset: magnification of rise phase.

G) Summary data illustrating similar amplitudes of D2-IPSCs across regions.

H) D2-IPSC amplitude normalized to the maximum outward current produced by dopamine (100 μM).

I) Lag to onset of D2-IPSCs (time to reach two s.d. above noise).

J) 10 – 90% rise time of D2-IPSCs.

K) Tau of decay of D2-IPSCs.
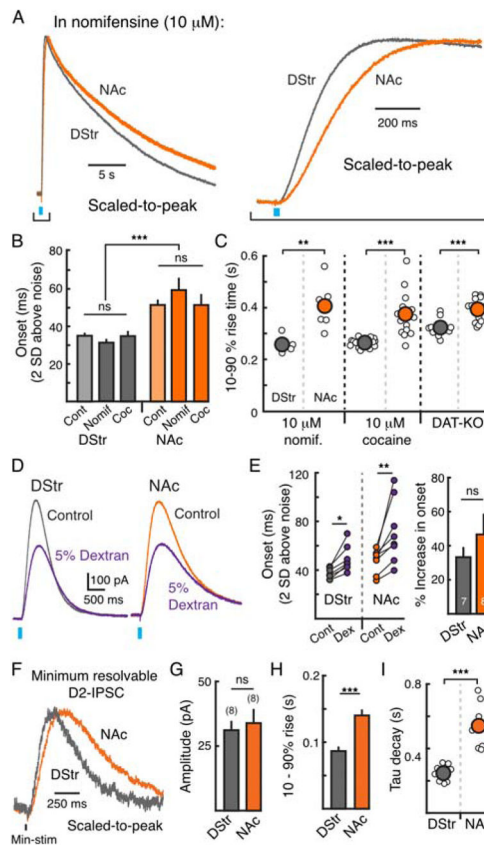
See also Supplemental Figure 1.

Figure 2. Role of reuptake, spillover and dopamine terminal density in regulating the synaptic activation of D2-receptors in the DStr and NAc

A) Average traces (magnified and scaled-to-peak) of light evoked D2-IPSCs in the DStr (gray, n = 5) and NAc (orange, n = 6) in the presence of nomifensine (10 μM). Right: magnification of the rise phase.

B) Lag to onset (time to reach two s.d. above the noise) for control IPSCs (light bars, from Figure 1I) and IPSCs in the presence of cocaine (10 μM) and nomifensine (10 μM).

C) 10 – 90% rise time of D2-IPSCs in nomifensine (10 μM, left), cocaine (10 μM, middle) and DAT-KO mice (right).

D) Representative traces in DStr and NAc medial shell (DStr - gray, NAc - orange) before and after slowing diffusion through the extracellular space with dextran (5% w/v, 35,000 – 50,000 kDa, purple traces).

E) Slowing diffusion with dextran prolonged the lag to onset (time to two s.d. above the noise) of D2-IPSCs in the DStr and NAc. Right: There was no difference in the percent change in the onset between regions (Mann-Whitney test; p = 0.2).

F) Representative traces of minimum resolvable D2-IPSCs in the DStr and NAc.

G) Amplitude of min-IPSCs.

H) 10 – 90% rise time of min-IPSCs.

I) Tau of decay of min-IPSCs.
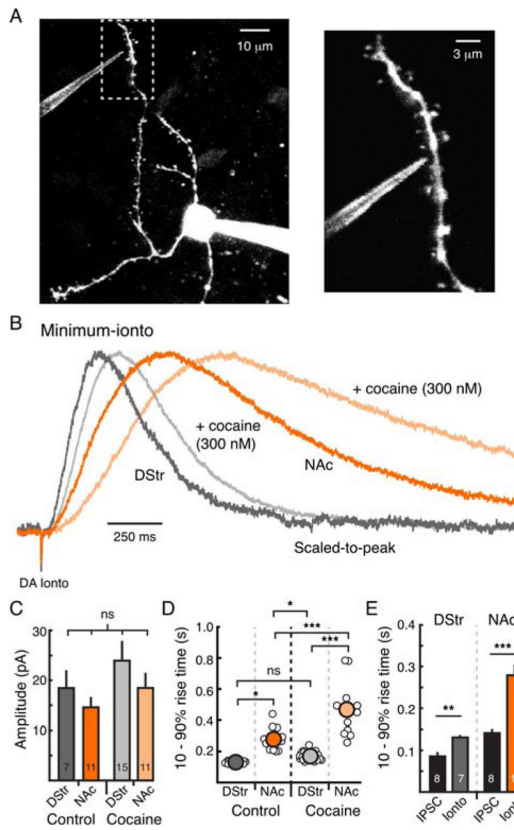
See also Supplemental Figure 2.

Figure 3. Postsynaptic D2-receptor signaling is slower in the NAc medial shell than the DStr

A) 2-photon image of a GIRK2^{+} MSNs filled with Alexa Fluor 594 (1 μM) and iontophoretic pipette filled with dopamine (1 M) and sulforhodamine 101 (300 μM).

B) Average traces of minimum D2-receptor mediated GIRK currents (minimum-ionto, scaled-to-peak) in the DStr (control, dark gray, n = 7) and NAc medial shell (control, dark orange, n = 11). Currents evoked in the presence of cocaine (300 nM) are shown in light gray (DStr, n = 15) and light orange (NAc, n = 11).

C) Amplitude of minimum-ionto in all four conditions.

D) 10 – 90% rise time of minimum-ionto in all four conditions.

E) Comparison of 10 – 90% rise time between minimal postsynaptic GIRK currents (Min-Ionto, from Figures 4B and 4D) and minimal stimulation IPSCs (min-IPSCs, from Figures 2G – 2J).
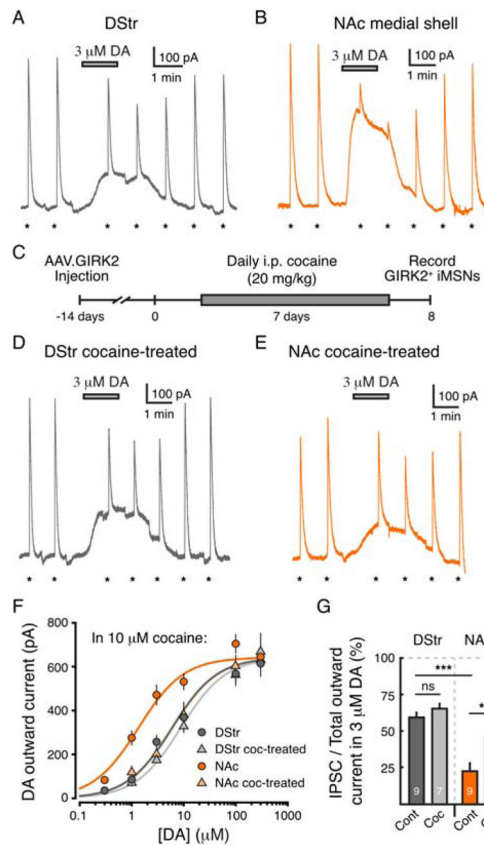
Figure 4. D2-receptors of the NAc medial shell have higher sensitivity for dopamine, which shifts in response to in vivo cocaine exposure

A – B) Representative whole-cell recordings from GIRK2^{+} MSNs in the DStr (gray, A) and NAc medial shell (orange, B). D2-IPSCs were evoked once per minute (indicated by *) while dopamine (3 μM) was bath applied. Recordings were made in the presence of cocaine (10 μM with DHβE, 1 μM).

C) Schematic of the timeline of AAV injection and chronic cocaine administration. Two weeks following AAV.GIRK2 injection, mice were treated with cocaine (20 mg/kg, i.p.) for 7 days and sacrificed for recordings on the 8th day.

D – E) Same as A and B showing representative traces of whole-cell recordings in GIRK2^{+} MSNs of the DStr (gray, D) and NAc medial shell (orange, E) in cocaine-treated mice.

F) Concentration-response curves for dopamine in slices from DStr and NAc (DStr, dark gray circles, EC_{50} = 5.9 μM, n = 46; NAc, dark orange circles, EC_{50} = 1.3 μM, n = 45; two-way ANOVA; p < 0.001). Following treatment with cocaine (as in C), the concentration-response curve in the DStr does not change (light gray triangles, EC_{50} = 8.8 μM, n = 38; two-way ANOVA vs. DStr control; p = 0.7) but the NAc curve shifts to the right (light orange triangles, EC_{50} = 6.1 μM, n = 28; two-way ANOVA vs. NAc control; p < 0.001).

G) Quantification of the ratio of phasic IPSC (evoked at the peak of the outward current) to total outward current (outward current in 3 μM dopamine + amplitude of IPSC evoked at peak of standing outward current).
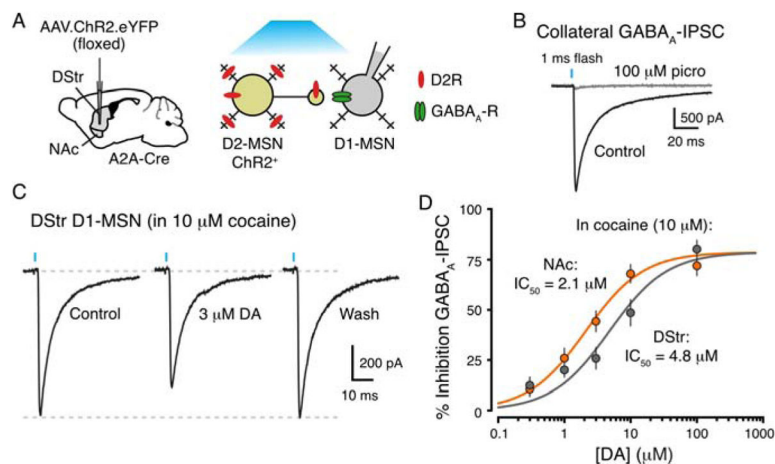
Figure 5. Axonal D2-receptors regulating collateral transmission have higher sensitivity in the NAc medial shell

A) Left: Schematic of the injection of AAV5.EF1a. DIO.hChR2(H134R)-EYFP.WPRE.hGH into the DStr and NAc of Adora2a-Cre (A2A-Cre) transgenic mice. Right: Cartoon schematic of the experimental setup. ChR2 is selectively expressed in D2-MSNs and blue light is used to evoke GABA release onto neighboring D1-MSNs.

B) Optogenetic stimulation of D2-MSNs (1 ms pulse, 470 nm, ~1.0 mW) evokes $GABA_A$-IPSCs on D1-MSNs which are blocked by the $GABA_A$-receptor antagonist picrotoxin (100 μM). Recordings were performed at −60 mV with a high Cl⁻ internal solution.

C) Representative whole-cell recording from a D1-MSN in the DStr. Dopamine (3 μM) produced an inhibition of the $GABA_A$-IPSC, which reversed following dopamine washout. Recordings were made in the presence of cocaine (10 μM), SCH 23390 (1 μM), scopolamine (200 nM), DNQX (10 μM), CGP 55845 (300 nM), and DHβE (1 μM).

D) Concentration-response curves for the inhibition of the $GABA_A$-IPSC by dopamine in slices from DStr and NAc (DStr, gray, IC_{50} = 4.8 μM, n = 37; NAc, orange, IC_{50} = 2.1 μM, n = 27; two-way ANOVA: p < 0.05). There was no regional difference in the maximal inhibition produced by dopamine between DStr and NAc (Mann-Whitney test; p = 0.3).
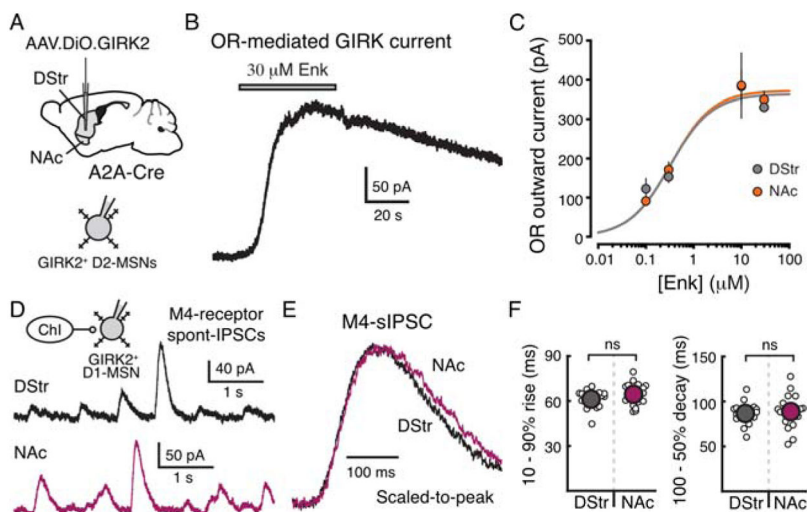
Figure 6. Other striatal GPCRs do not exhibit regional differences in sensitivity or kinetics

A) Upper: Schematic of the injection of AAV2/9.hSyn.DIO.tdTomato.GIRK2 into the DStr and NAc of A2A-Cre transgenic mice. Lower: Recording schematic.

B) Representative recording from a GIRK2$^+$ D2-MSN showing a GIRK current resulting from application of leu-enkephalin (30 μM).

C) Concentration-response curves for the opioid receptor (OR) mediated GIRK currents in slices from DStr and NAc (DStr, gray, EC_{50} = 320 nM, n = 37; NAc, orange, EC_{50} = 340 nM, n = 27; p = 0.9, two-way ANOVA).

D) Representative whole-cell recording showing spontaneous M4 muscarinic IPSCs (M4-sIPSCs) in the DStr (top) and NAc medial shell (bottom). Inset: schematic of the microcircuit connecting a cholinergic interneuron (ChI) and GIRK2$^+$ direct pathway MSN (D1-MSN).

E) Representative traces (overlaid and scaled-to-peak) of M4-sIPSCs in the DStr (black) and NAc (magenta). Spontaneous events were detected and averaged across each cell.

F) 10 – 90% rise time and 100 – 50% decay time of M4-sIPSCs in the DStr (n = 13) and NAc (n = 15).

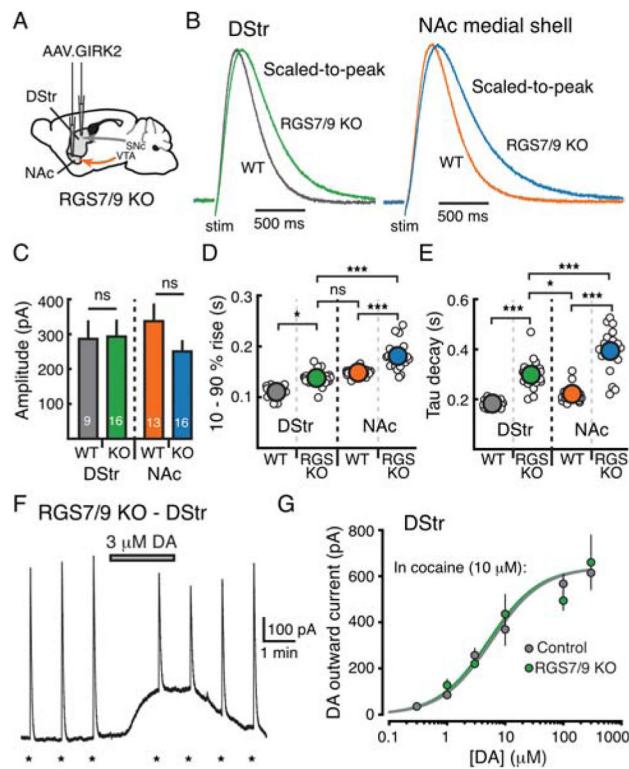See also Supplemental Figure 3 and Supplemental Figure 4.

Figure 7. RGS proteins regulate the timing but not the sensitivity of D2-receptor activation

A) Injection schematic of RGS7/9 double knock-out (RGS7/9 KO) mice injected with AAV.GIRK2 in the DStr and NAc.

B) Average traces of D2-IPSCs in the DStr (left) and NAc (right) from RGS7/9 KO mice (DStr: green, NAc: blue) and control littermates (DStr: gray, NAc: orange).

C) Quantification of amplitude of IPSCs in all four groups.

D) Quantification of 10 – 90% rise time in all four groups.

E) Quantification of tau of decay in all four groups.

F) Representative whole-cell recording from GIRK2+ MSN in the DStr of RGS7/9 KO mice. D2-IPSCs were evoked once per minute (indicated by *) while dopamine (3 μM) was bath applied, as in Figure 4A. Recordings were made in the presence of cocaine (10 μM with DHβE, 1 μM).

G) Concentration-response curves for the dopamine-mediated GIRK currents in slices from RGS7/9 KO mice compared to control (control, from Figure 4F: EC_{50} = 5.9 μM; RGS7/9KO: EC_{50} = 6.7 μM; two-way ANOVA; p = 0.8).
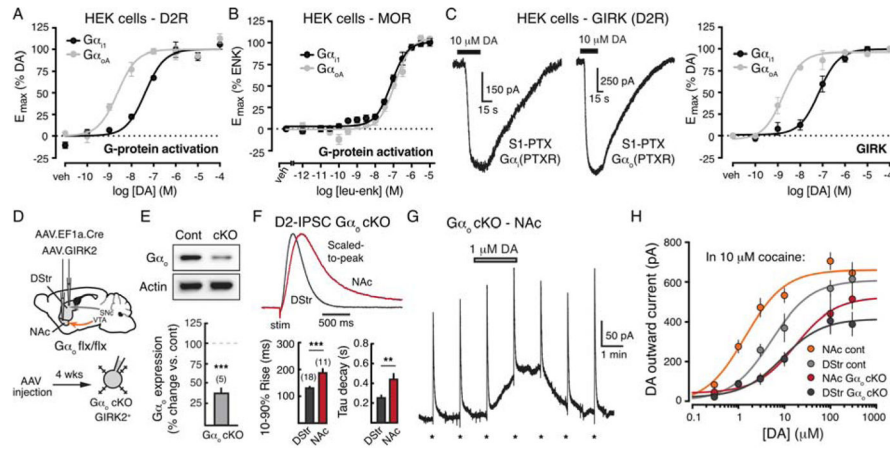
See also Supplemental Figure 5.

Figure 8. Gα subunit contribute to regional differences in D2-receptor sensitivity

A) Concentration-response curves for the dopamine-mediated D2 receptor-dependent G-protein activation in HEK cells.

B) Concentration-response curves for the leu-enkephalin-mediated MOR receptor-dependent G-protein activation in HEK cells.

C) Dopamine mediated GIRK currents in HEK cells with D2 receptors coupled to either $G\alpha_{i1}$ (left trace) or $G\alpha_{oA}$ (right trace). Right: concentration-response curves for the dopamine-mediated activation of GIRK currents in HEK cells.

D) Top: Schematic of the injection of AAV.EF1a.Cre and AAV.GIRK2 into the DStr and NAc of $G\alpha_o$ flx/flx transgenic mice. Bottom: Recording schematic showing conditional elimination of $G\alpha_o$ ($G\alpha_o$ cKO) in GIRK2^{+} MSNs 4 weeks after AAV injection.

E) Top: Western blot showing reduction in $G\alpha_o$ protein and actin controls in striatal tissue. Bottom: Quantification of $G\alpha_o$ protein levels in striatal tissue from $G\alpha_o$ cKO mice, normalized to control hemispheres.

F) Top: Representative whole-cell recordings of D2-IPSCs in the DStr (gray) and NAc (orange) of $G\alpha_o$ cKO mice. Bottom: Quantification of 10 – 90% rise time (left) and tau of decay (right) in $G\alpha_o$ cKO mice.

G) Representative whole-cell recording from a GIRK2^{+} MSN in the NAc of $G\alpha_o$ cKO mice. D2-IPSCs were evoked once per minute (indicated by *) while dopamine (1 μM) was bath applied. Recordings were made in the presence of cocaine (10 μM) with DHβE (1 μM) to block nicotinic receptors.

H) Concentration-response curves for the dopamine-mediated GIRK currents in slices from $G\alpha_o$ cKO mice compared to control (DStr control, from Figure 4F: EC_{50} = 5.9 μM; DStr $G\alpha_o$ cKO: EC_{50} = 7.5 μM, n = 33; NAc control, from Figure 4F: EC_{50} = 1.3 μM; NAc $G\alpha_o$ cKO: EC_{50} = 11.7 μM, n = 32).

See also Supplemental Figure 6.